Environment International 200 (2025) 109535

Contents lists available at ScienceDirect

Environment International

journal homepage: www.elsevier.com/locate/envint

Full length article

Development and validation of a gridded emissions inventory for HFC-134a in China

Jing Wu [a,b,1,*], Tong Wang [a,1], Minde An [c,d,1], Shan Ding [e], Bo Yao [f,g], Luke M. Western [d], Pallav Purohit [h], Zehua Liu [i], Zechen Zhang [j], Lin Peng [a,b,*]

[a] School of Environment, Beijing Jiaotong University, Beijing 100044, China
[b] Institute of Transport Energy and Environment, Beijing Jiaotong University, Beijing 100044, China
[c] Center for Sustainability Science and Strategy, Massachusetts Institute of Technology, Cambridge, MA, USA
[d] School of Chemistry, University of Bristol, Bristol BS8 1TS, UK
[e] The MOE Key Laboratory of Resource and Environmental System Optimization, College of Environmental Science and Engineering, North China Electric Power University, Beijing 102206, China
[f] Meteorological Observation Centre of China Meteorological Administration (MOC/CMA), Beijing 100081, PR China
[g] Department of Atmospheric and Oceanic Sciences & Institute of Atmospheric Sciences, Fudan University, Shanghai, China
[h] International Institute for Applied Systems Analysis (IIASA), Schlossplatz 1, A-2361 Laxenburg, Austria
[i] Beijing Jingcheng Machinery & Electricity Company, Beijing 100027, China
[j] Chinese Acad Environm Planning, State Environm Protect Key Lab Environm Pollut & G, Beijing 100041, PR China

ARTICLE INFO

Handling Editor: Xavier Querol

Keywords:
HFC-134a
Gridded emission inventory
Global warming
Trifluoroacetic acid
Kigali Amendment

ABSTRACT

1,1,1,2-Tetrafluoroethane (HFC-134a), a potent greenhouse gas, breaks down to form trifluoroacetic acid (TFA). Lack of its gridded emissions inventories makes it difficult to analyze the spatial distribution of emissions. This study developed a framework for national and gridded HFC-134a bank and emission calculations, validation and environmental impact assessments. Within this framework, we used production and consumption data along with emission factors to compile a gridded inventory for China. The results reveal an increase in national HFC-134a emissions, from 0.1 kt yr^{-1} in 1995 to 48 kt yr^{-1} in 2020, with banks also increasing from 0.9 to 301 kt. Guangdong, Jiangsu, and Shandong provinces showed the largest cumulative emissions, totaling 98 kt between 1995 and 2020, representing 28% of HFC-134a national emissions. A Lagrangian dispersion model, in conjunction with atmospheric observations, was used to validate the gridded inventory, where the simulations based on the gridded inventory were in reasonable agreement with the observations. A carbon–neutral (CN) scenario was developed to project future emissions. The adoption of HFO-1234yf and R-513A as substitutes for HFC-134a is projected to cause an additional 701 kt of cumulative TFA formation potential between 1995 and 2060, on top of the 3825 kt projected under the Kigali Amendment scenario.

1. Introduction

Hydrofluorocarbons (HFCs) have been widely used as the main replacements for ozone-depleting substances (ODS) controlled under the Montreal Protocol (UNEP, 2020). Many HFCs are potent greenhouse gases and are subject to a global phase-down under the Kigali Amendment (KA) to the Montreal Protocol (Purohit et al., 2022). While the Kyoto Protocol initially aimed to reduce HFC emissions, these efforts are now being pursued under the Paris Agreement of the United Nations Framework Convention on Climate Change (UNFCCC). The Kigali Amendment to the Montreal Protocol was adopted in 2016 and entered into force from 1 January 2019. It aims to regulate both the production and consumption of HFCs (UNEP, 2020). This means that countries that ratify the amendment are obligated to gradually reduce the amount of HFCs they produce and use. As of March 2025, 163 signatories have ratified the Kigali Amendment to the Montreal Protocol, which aims to phase down HFCs worldwide (UN, 2025).

1,1,1,2-Tetrafluoroethane (CH_2FCH_3, HFC-134a) has an atmospheric lifetime of 14 years, a direct radiative efficiency of 0.167 W m^{-2} ppb^{-1}, and global warming potential (GWP) of 1530 over a 100-year time

* Corresponding authors.
E-mail addresses: wujing.108@163.com (J. Wu), penglin6611@163.com (L. Peng).
[1] These authors have contributed equally to this work and share first authorship.

https://doi.org/10.1016/j.envint.2025.109535
Received 6 December 2024; Received in revised form 12 May 2025; Accepted 14 May 2025
Available online 17 May 2025

horizon (Smith et al., 2021). Following the phase-out of the production of most long-lived ODSs in 2010, the global emissions and atmospheric abundance of HFC-134a increased rapidly, rising from 177 Gg yr^{-1} and 67 ppt in 2012 to 245 Gg yr^{-1} and 113 ppt in 2020 (WMO, 2023). Consequently, the radiative forcing attributed to HFC-134a reached 19.5 mW m^{-2} in 2020 (WMO, 2023). HFC-134a can also generate the degradation product trifluoroacetic acid (TFA) at yields of approximately 7% to 21% (Kotamarthi et al., 1998; Luecken et al., 2010), which can impact aquatic ecosystems. The no-observed effect concentration (NOEC) value for the inhibition of algal growth was 120 μg L^{-1} (Berends et al., 1999). Studies have observed a significant increase in TFA concentration in water and plants across Europe and China over the last decade (Zhai et al., 2015; Freeling et al., 2022). While current evidence on major TFA risks to humans or the environment remains limited, its persistence and continuing emissions could cause significant environmental accumulation. This widespread, long-lasting contamination may become irreversible, posing challenges if future research uncovers adverse effects (Garavagno et al., 2024). At present, the primary low-GWP alternative to HFC-134a in the mobile air conditioning sector is HFO-1234yf ($CF_3CF{=}CH_2$, GWP<1). With an atmospheric lifetime of only 12 days (WMO, 2018) and a TFA yield of 100% (Luecken et al., 2010), HFO-1234yf will generate more TFA rapidly than HFC-134a (Luecken et al., 2010; David et al., 2021).

To assess the environmental impact of HFC-134a on climate change and TFA formation potential, accurate emission estimates are necessary. Most bottom-up studies, which rely on production and consumption data, employ the Tier 2a method at the sub-application level, utilizing disaggregated data and specific emission factors for distinct equipment types (IPCC, 2006). In contrast, only a few studies (Fang et al., 2016, 2018) have used the Tier 1a method at the application level, which relies on aggregated data and composite factors, resulting in lower precision compared to Tier 2a. The most recent relevant study, conducted by Yi et al. (2023), covers a wide range of sectors, including the mobile air conditioning (MAC) sector, the commercial air conditioning sector, the foam sector, the metered-dose inhaler sector, and the production sector. Most of the existing bottom-up studies only estimated total HFC-134a emissions at regional (Harnisch et al., 2002; Ding et al., 2023) or national (Godwin, 2012; Fang et al., 2016, 2018; Sharma et al., 2017; Li et al., 2019; Xiang et al., 2022; Bai et al., 2023; EDGAR, 2023; Wu et al., 2023; Yi et al., 2023) scales. Only Yi et al. (2023) has also estimated city-level emissions, specifically for Beijing, Guangzhou, Hangzhou and Lanzhou in China. For the MAC sector, they used city-level vehicle ownership data for emission calculations. For other sectors, city-level emissions were calculated by identifying the socio-economic parameter that is most relevant to emissions and using that parameter's share of the national total to the specific city. For ODSs and fluorinated greenhouse gases, only one gridded inventory has been published, which is for HCFC-22 by Wu et al. (2022). The results of this inventory have not been validated using observational data in conjunction with an atmospheric transport model. As for banks (HFC-134a that has been produced but not yet released to the atmosphere or destroyed), only a limited number of studies have documented global or national banks of HFC-134a (Velders et al., 2014; Montzka et al., 2015; Wu et al., 2023; Bai et al., 2023). The lack of gridded data on banks and emissions poses challenges in analyzing the spatial distribution of banks and emissions, assessing regional contributions, and identifying gridded locations with the highest HFC-134a emissions. High spatial resolution emission inventories can provide key input data for atmospheric simulation models, which can improve modeling accuracy.

China is the world's leading producer, consumer, and emitter of HFCs, contributing 46% of the global HFCs production in 2022 (UNEP, 2024). HFCs produced in China satisfy both domestic consumption needs and international export demands. The share of global HFC-134a emissions attributable to China increased significantly, from 1% in 1995 to 20% in 2020 (WMO, 2023). China pledged to a carbon neutrality target by 2060 in 2020 (People's Government of the People's Republic of China, 2021; Zhang et al., 2022) and ratified the Kigali Amendment in 2021, recognizing the necessity to reduce HFC production and consumption. Bai et al. (2023) conducted a study outlining a pathway to reduce HFCs emissions in alignment with China's 2060 carbon neutrality objective, which highlighted potential challenges in phasing down HFC-134a due to rising consumption demands and the selection of optimal alternatives. To address these challenges, in this study, we have developed a comprehensive modelling framework for national-gridded bank and emission calculations, validation and environmental impact assessments (GEVE) as illustrated in Fig. 1. Five emission sources associated with the production and consumption of HFC-134a were analyzed, leading to the development of a methodology for computing a gridded bank and emission inventory. Using the GEVE framework, this study compiled a gridded (1°×1°) bank and emission inventory of HFC-134a in China for the period from 1995 to 2020. It analyzed the spatial distribution characteristics and identified the grid cells with the highest emissions. The gridded emission inventory has been validated against observed atmospheric mole fractions of HFC-134a from nine different measurement sites across China, using an atmospheric transport model, namely the Numerical Atmospheric-dispersion Modelling Environment (NAME) (Jones et al., 2007). In this study, a carbon–neutral scenario was developed to accelerate the phase-down of HFC-134a in accordance with the phase down schedule of the Kigali Amendment. The emission reduction potentials of HFCs by 2060 were then analyzed under three scenarios, along with their associated environmental impacts, including the potential to form TFA.

2. Methods

2.1. Estimation of HFC-134a national bank and emission based on material flow analysis

Emission sources of HFC-134a in China were identified, stemming from four consumption processes and one fluorine chemical production process: (1) the mobile air conditioning (MAC) sector, (2) the industrial and commercial refrigeration (ICR) sector, (3) the foam sector, (4) miscellaneous consumption sectors, and (5) the production sectors. The material flow analysis method was used to identify these emission processes, with the material flow topology provided in Fig. S1. Section 1 of the Supplementary Information (SI) describes the specific meaning of each emission process within each sector and provides the reference source for the classification of HFC-134a in the consumption sector.

For the foam sector, the emissions factor and longevity of emissions depends on the waste disposal method. If the foam product is disposed of in a landfill, it may emit HFC-134a for more than 10 years beyond its service life. If incinerated, HFC-134a undergoes complete pyrolysis and is no longer emitted into the atmosphere (Roh et al., 2019). Disposal methods for foam products may vary regionally. However, due to limited data availability, obtaining more detailed sub-regional data is challenging. Therefore, this study relies on national landfill and incineration ratios for calculations, with 64% of foam products disposed of in landfills and 36% incinerated (National Bureau of Statistics of China, 2020). Therefore, throughout the entire lifecycle of foams, two distinct banks exist: an active bank (foams in use) and an inactive bank (post-disposal), often referred as the waste bank. In the foam sector, active banks refer to HFC-134a in currently installed insulation products (PU and XPS) with ongoing emission potential, while inactive banks refer to retired foam materials containing stabilized HFC-134a that are awaiting disposal or degradation. This study updated and improved the estimation of inactive banks and waste disposal emissions building on the IPCC's Method 1a (IPCC, 2006). For the MAC and ICR sectors, this study provisionally assumed that after the product reached service life, the residual refrigerant in products would be entirely emitted to the atmosphere. It solely accounted for active banks, referring to the remaining banks of fluorinated greenhouse gases still existing throughout the lifecycle of the products. This is due to the fact that, despite that some

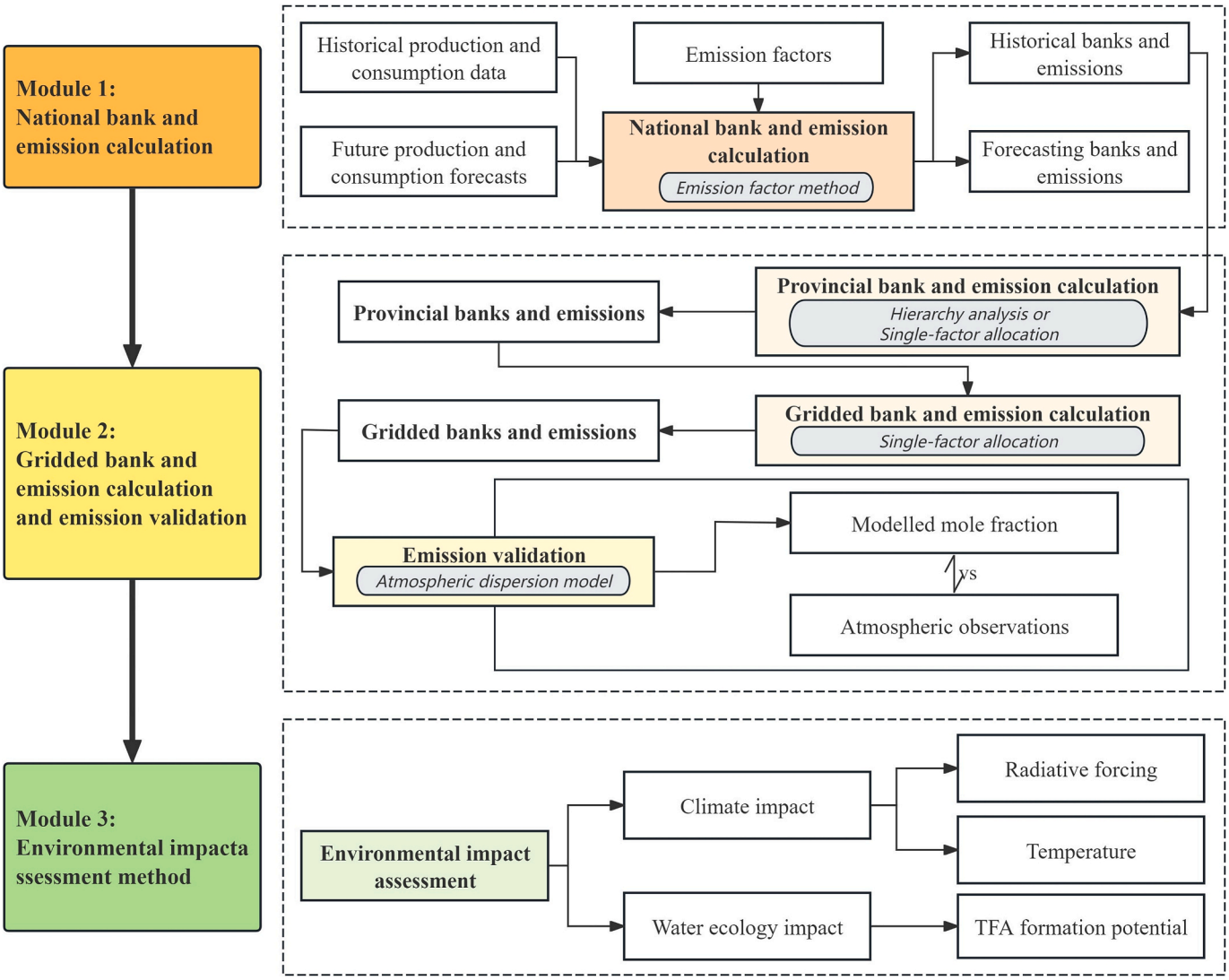

Fig. 1. Modeling framework for national-gridded bank and emission calculations, gridded emissions validation and environmental impact assessments (GEVE).

Chinese enterprises have recently started refrigerant recycling efforts in the MAC and ICR sectors, they have been unable to collect data on the quantities of the recovered refrigerant. Detailed information on banks, emission calculation methods, emission factors and activity data for all sectors is available in Tables S1–S4 (Section 1 of the SI). The calculations of production and consumption used for the forecast are detailed in section 3 of the methodology. It should be noted that, due to data unavailability, Hong Kong, Macao and Taiwan were not included in the inventories calculated in this study.

To estimate the uncertainty in HFC-134a emission, a Monte Carlo simulation was conducted, accounting for uncertainties in initial consumption, emission factors, radiative efficiency, and climate sensitivity parameters. The uncertainty calculations were performed using Excel, assuming a 10% uncertainty for activity data and emission factors in each sector (e.g., Wu et al., 2022, 2023). Following Wei (2011), the probability density distribution functions for activity level data and emission factors were modeled using a lognormal distribution. The Monte Carlo analysis included 100,000 simulations, with the uncertainty range of HFC-134a emissions expressed as 10% and 90% confidence intervals (Wu et al., 2022, 2023).

2.2. HFC-134a gridded bank and emission calculation and gridded emission validation

In this study, following the calculations of aggregated national HFC-134a bank and emission inventories, either the single-factor allocation method or the hierarchy analysis method was used to calculate the provincial-gridded banks and emissions. The single-factor allocation methodology identifies factors potentially relevant to banks or emissions from a sector and selects the most relevant parameter. National banks and emissions are then distributed to provinces based on each province's share of that parameter (Wu et al., 2022). When emissions from a sector are affected by various factors, the single-factor allocation method becomes inadequate. Instead, hierarchical analysis is used to perform a multi-factor assessment, determining the relative significance of these factors (Wang, 2018). Notably, the provincial and gridded inventory of HFC-134a developed in this study did not account for production emissions because annual production data for each HFC-134a production enterprise was unavailable. Our calculations indicate that production emissions constitute a minor portion of total emissions, accounting for only 2% in 2020.

For both the MAC and miscellaneous consumption sectors, a correlation analysis was conducted using SPSS statistics to examine the relationship between yearly national emissions and relevant proxy parameters, across each stage of the processes' life cycle (Fig. 2). The most

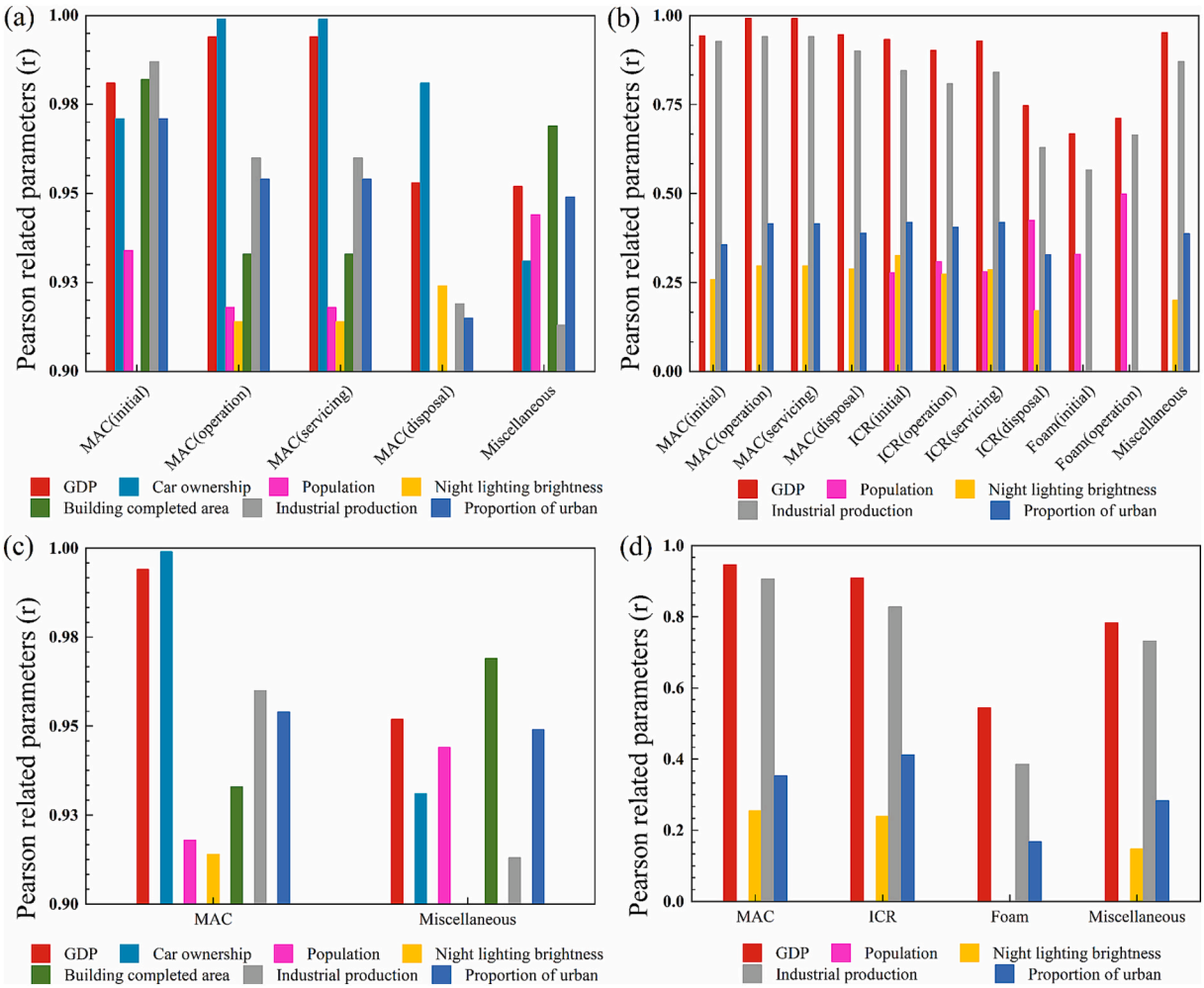

Fig. 2. Pearson correlation coefficient between emissions and related parameters: (a) national emissions and related parameters of MAC and miscellaneous consumption sectors over a yearly period; (b) provincial emissions and related parameters for each sector; (c) national banks and related parameters for MAC and miscellaneous consumption sectors over a yearly period; (d) provincial banks and related parameters for each sector.

relevant parameters were then selected as provincial allocation parameters. Industrial production ($r=0.99$, $p<0.01$) and car ownership ($r=0.98$–0.99, $p<0.01$) were selected as the provincial allocation parameter for initial emissions and other emission processes (operation, servicing and disposal emissions) within the MAC sector. In the miscellaneous consumption sectors, building completed area ($r=0.97$, $p<0.01$) was selected as the allocation parameter (Fig. 2a). A similar analysis was conducted for banks, car ownership ($r=0.99$, $p<0.01$) and building completed area ($r=0.97$, $p<0.01$) were selected as the provincial bank allocation parameter for MAC and miscellaneous consumption sectors (Fig. 2c). In the foam sector, limited historical emission data were available for the correlation calculations, primarily due to the adoption of HFC-134a around 2016 as a blowing agent in China. Therefore, building completed area was chosen as the provincial allocation parameter for this sector, based on findings from the study by Wu et al. (2022) on HCFC-22. In the ICR sector, we adopt the hierarchy analysis method as outlined by Yang (2010) to calculate provincial banks and emissions. Detailed data sources are provided in Table S2.

Using provincial HFC-134a banks and emissions as a basis, this study applied the single-factor allocation method to compute a gridded inventory at a resolution of $1°\times1°$. The factors in Fig. 2b and 2d were selected as potential allocation variables for calculating the gridded inventory (Aucott et al., 1999; Doll et al., 2000; Papasavva et al., 2009). Correlations between provincial emissions and these three parameters were calculated for every emission process in every sector to determine the best proxy for gridded emissions (see Fig. 2b). It was found that GDP ($r=0.67$–0.99, $p\leq0.01$) showed strong correlation with emission estimates across all emission processes in all sectors. Therefore, GDP was selected as the gridded allocation parameter for calculating HFC-134a gridded emissions. Similarly, a correlation analysis was performed between the banks and the associated parameters, and GDP ($r=0.54$–0.95, $p\leq0.01$) was selected as the allocation parameter for the calculation of the HFC-134a gridded banks. As a result, gridded ($1°\times1°$) GDP data was used as a proxy to allocate provincial emissions to the grids, which was implemented using ArcGIS. It is worth noting that correlation does not imply causation, which could introduce errors or uncertainties in the gridded emissions. However, our validation using a Lagrangian dispersion model is useful for assessing the reliability of the emission inventory.

The gridded emissions of HFC-134a compiled in this study were validated using atmospheric observations of HFC-134a combined with an atmospheric dispersion model. The atmospheric observations of HFC-134a mole fractions used for verification were obtained from a network operated by the China Meteorological Administration, comprising nine sites across different regions of China from 2011 to 2020. Table S5 of the SI contained complete sampling information of the measurements. A Lagrangian particle dispersion model, namely the Numerical Atmospheric-dispersion Modelling Environment (NAME) (Jones et al., 2007) from the UK Met Office was used to derive the sensitivity of the atmospheric observation to emissions in each grid (or in other words the

contribution from emissions in each grid to the observations). Detailed information about the set-up of the NAME backwards run can be found in An et al. (2023, 2024). The gridded inventory of HFC-134a compiled in this study was combined with the emissions contribution from each grid to simulate the mole fractions made at the observation sites using the NAME model. Emissions outside China are assumed to be zero during the simulation. Baseline mole fractions were simulated by considering the sensitivities of observations to the domain boundaries, as output by the NAME model. Background mole fractions at the domain boundaries were obtained from the AGAGE 12-box assimilation of global background measurements (Rigby et al., 2013, WMO, 2023). By comparing the simulated mole fractions (baseline plus enhancements) with the observed mole fractions at the nine sites, we assessed the reliability of the gridded emissions.

This study used several statistical criteria to evaluate the agreement between simulated and observed mole fractions at the stations, including the normalized mean bias (NMB) and normalized mean error (NME) (Emery et al., 2001). Further details on NMB and NME can be found in Section 2 of SI.

2.3. HFC-134a emission reduction scenarios and environmental impact assessment

In this study, three scenarios were developed: the Pre-Kigali Amendment (Pre-KA) scenario, the Kigali Amendment (KA) scenario, and the Carbon Neutrality (CN) scenarios. These scenarios were devised to assess the potential for emission reductions and the environmental impacts of HFC-134a, as detailed below:

1) The Pre-KA scenario represents a situation where HFC-134a is not subjected to any phase-down. Based on the GAINS (Greenhouse Gas and Air Pollution Interactions and Synergies Model) methodology (Purohit and Höglund-Isaksson, 2017; Purohit et al., 2020), we projected future production and consumption demands across various sectors for the pre-Kigali scenario and used this data to estimate future emissions. By analyzing the relevant parameters, the production sector, MAC, and foam sector use GDP to project production and consumption for 2020–2060, in accordance with the methodologies outlined in Li et al. (2019). The ICR sector and miscellaneous consumption sectors use public building completed area to forecast consumption for 2020–2060. The results of the Pearson correlation coefficient of the activity data for each sector are shown in Table S10 of the SI. According to the International Council on Clean Transportation (ICCT) projected value of car ownership in China with HFC as a refrigerant (Jin et al., 2021), per capita car ownership is expected to keep rising until 2060. As a result, this study does not set a saturation value for car consumption.
2) The KA scenario involves a phased reduction of HFC-134a usage according to the Kigali Amendment's schedule. This includes a 10% reduction by 2029, 30% by 2035, 50% by 2040 and 80% by 2045 from China's baseline;
3) The CN scenario addresses the need to achieve carbon neutrality by 2060, given that the KA scenario reduces HFC-134a consumption to only 80% of the baseline level by 2045 (Bai et al., 2023). To allow for a time buffer towards switching to low-GWP alternatives, a CN scenario was developed to maximize the demand for HFC-134a consumption in China while still achieving the emission reduction target.

In this study, the CN scenario was developed using a nonlinear programming approach to accelerate the phase-down of HFC-134a consumption under the KA scenario while meeting the highest possible demand for HFC-134. The objective function is defined as the maximum consumption of HFC-134a between 2040 and 2060. In order to reasonably set the 2060 HFC-134a emission target, this study refers to the emission proportion of China's HFCs from the Shared Socioeconomic Pathway (SSP) published by CMIP6 (Gidden et al., 2019), to set the range of China's HFC-134a emission target under the 2060 carbon neutrality goal. The key parameters affecting HFC-134a emissions in 2060 are the reduction rate in 2040 and 2045, as well as the reduction rate from 2045 to 2060, which were adjusted in the dynamic planning calculation. As most of the lifetime of HFCs-containing products does not exceed 20 years, it is assumed in this study that China will accelerate the phase-down of the consumption of HFC-134a after 2040. The objective function and constraints are as follows:

$$MAC(P) = \sum_{i=2040}^{2060} (C_{MAC,i} + C_{ICR,i} + C_{Foam,i} + C_{other,i})$$

$$E_{MAC,2060} + E_{ICR,2060} + E_{Foam,2060} + E_{Other,2060} \leq E_{CN,2060}$$

$$C_{MAC,i} + C_{ICR,i} + C_{Foam,i} + C_{other,i} \leq K_i$$

$$C_{2040} > 0$$

$$C_{2045} > 0$$

$$C_{2045+} > 0$$

$C_{MAC,i}$, $C_{ICR,i}$, $C_{Foam,i}$ and $C_{other,i}$ are the consumption in year i for MAC, ICR, Foam and miscellaneous consumption sectors respectively; $E_{CN,2060}$ is the maximum emission limitation of HFC-134a in 2060 under the CN scenario, which is based on the projected scenario in SSP1-2.6 of the Sixth Assessment Report of the IPCC (IPCC, 2021); $E_{MAC,2060}$, $E_{ICR,2060}$, $E_{Foam,2060}$ and $E_{Other,2060}$ are the emissions of HFC-134a in the MAC, ICR, foam and miscellaneous consumption sectors in 2060, respectively; K_i is the consumption limitation for year i as required by the Kigali Amendment; C_{2040}, C_{2045}, C_{2045+} are the reduction rates in 2040, 2045 and the average annual percentage of reductions after 2045, respectively. Fig. 3 presents the consumption phase-down schedules for each scenario.

In order to predict the TFA formation potential from HFC-134a and its substitutes, we assumed that all HFC-134a used in MAC and foam applications was replaced by HFO-1234yf, while HFC-134a used in the ICR sector was replaced by R-513A (56% HFC-1234yf, 44% HFC-134a). Miscellaneous consumption sectors were excluded due to the difficulty in identifying potential substitutes for HFC-134a in these sectors. The reasons for selecting HFC-134a alternatives and related information are detailed in Section 3 and Table S9 of SI.

In this study, we analyzed the environmental impacts of HFC-134a and its alternatives on global climate and water ecology under different emission reduction scenarios. The methods for calculating the

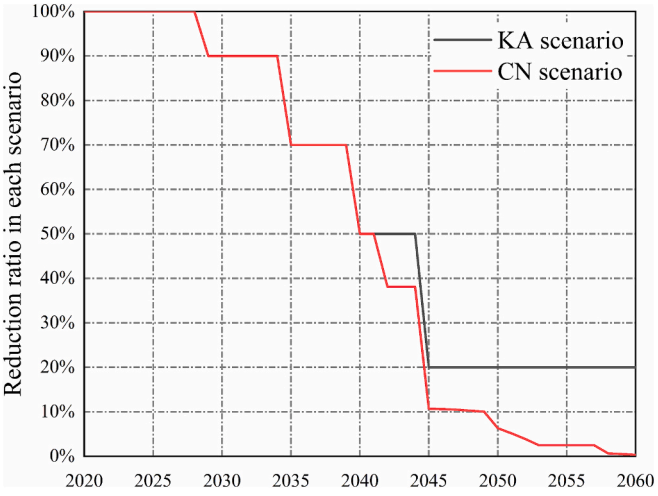

Fig. 3. HFC-134a consumption phase-down schedules under the Kigali Amendment and that proposed in the Carbon Neutrality (CN) scenario.

increased radiative forcing or temperature increase due to HFC-134a emissions, as a measure of climate impact, are based on Xu et al. (2013) and Fang et al. (2016). The amount of TFA formation potential during the atmospheric degradation of HFC-134a and its potential alternatives was used to roughly predict their ecological and environmental impacts on major catchment bodies. The calculations of TFA formation potential were based on Wu et al. (2014), with detailed calculations provided in Section 3 of the SI.

3. Results and discussion

3.1. HFC-134a historical banks, emissions, and environmental effects

As CFCs and HCFCs have been gradually replaced by HFC-134a in the refrigeration, air-conditioning and foam-consuming sectors, the production and consumption of HFC-134a in China have surged significantly. From approximately 1 kt yr^{-1} for both production and consumption in 1995, these figures escalated to 190 and 90 kt yr^{-1}, respectively by 2020. Over the period spanning 1995 to 2020, cumulative production and consumption reached 1,686 and 646 kt, respectively, as illustrated in Fig. 4. Simultaneously, banks also accumulated over time, reaching 301 kt by 2020. This resulted in a rapid increase in emissions, rising from less than 1 kt yr^{-1} in 1995 to 48 kt yr^{-1} (39–55 kt yr^{-1}) in 2020. The average annual growth rate was 29%, with cumulative emissions totaling 354 kt (294–412 kt). It is important to note that this study does not include data for Hong Kong, Macao and Taiwan. The emission data from these regions exhibit minimal impacts on the national emissions. For instance, as documented by the Ministry of Ecology and Environment of the People's Republic of China (2023), Hong Kong's HFC-134a emissions in 2018 constituted merely 1.6% of China's total emissions.

As indicated by Fig. 4a and c, the growth in HFC-134a emissions has begun to fall behind the growth in consumption since 1995, with cumulative emissions (354 kt) being lower than cumulative consumption (634 kt). This discrepancy is attributable to emissions generated throughout the life cycle of product manufacturing, service, and waste disposal associated with HFC-134a, leading to a buildup in the bank size and delayed emission from their year of consumption. Fig. 5 presents a comparison between the historical emissions estimated in this study and previously published HFC-134a emissions data from China (Yokouchi et al., 2006; Kim et al., 2010; Li et al., 2011, 2019; Fang et al., 2012, 2018, 2019; Yao et al., 2012, 2019; Lunt et al., 2015; Xie et al., 2019; Yi et al., 2021, 2023; Bai et al., 2023). The findings of this study closely align with recent bottom-up studies (Yi et al., 2023; Bai et al., 2023) and follow a similar trend. Moreover, they fall within the uncertainty range of the majority of existing research outcomes. As shown in Fig. 5, the uncertainty range of emission estimates has increased over time, primarily due to the increasing uncertainty of bank size. Factors such as the addition of new equipment, emissions during operation and maintenance, and equipment disposal significantly influence bank changes. The yearly variations in these factors, along with their cumulative impact, have contributed to the rising uncertainty in bank estimates.

Around 1995, the MAC sector in China adopted HFC-134a as a refrigerant. By 2020, the MAC sector accounted for the highest cumulative consumption, emissions, and banks among all sectors at 236 kt (37%), 136 kt (39%) and 113 kt (37%), respectively. This was followed by the miscellaneous consumption sectors and the ICR sector. In the analysis of each life cycle stage from 1995 to 2020, operating emissions of HFC-134a were consistently the highest, ranging from 41% to 57% of the total, whereas initial emissions consistently register the lowest

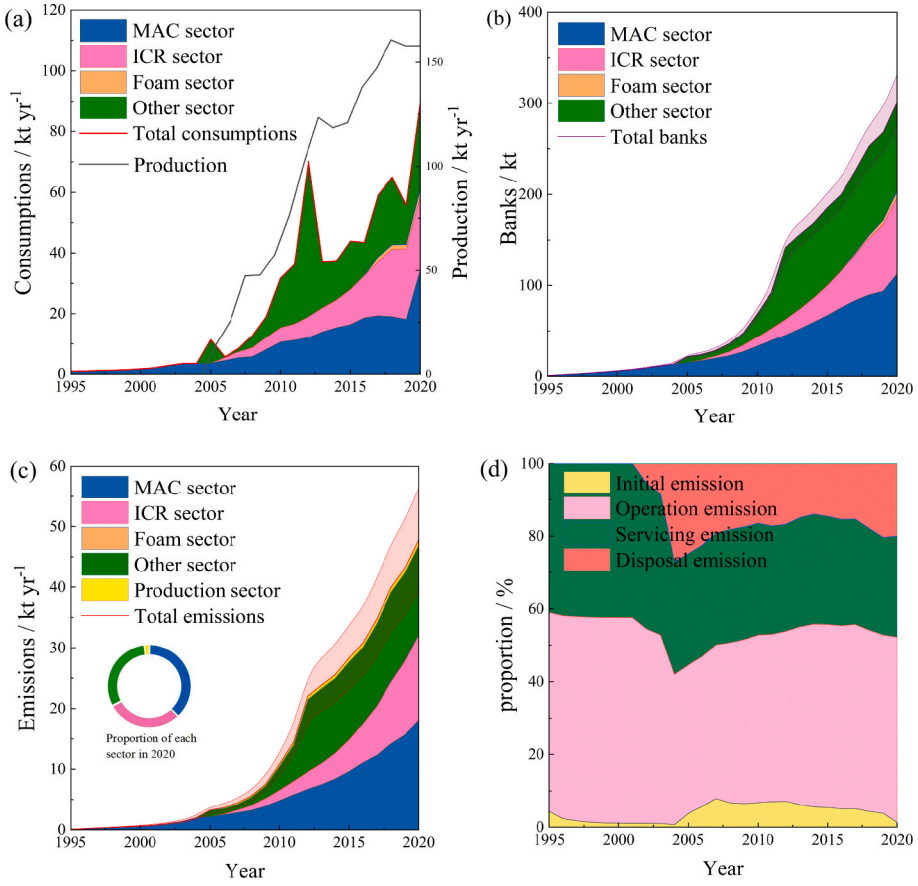

Fig. 4. HFC-134a historical consumption, production, banks and emission in each sector and each life cycle stage from 1995 to 2020: (a) Production and consumption (stacked graphic represents consumption); (b) Bank; (c) HFC-134a emissions in each sector; (d) proportion of emissions from each life cycle.

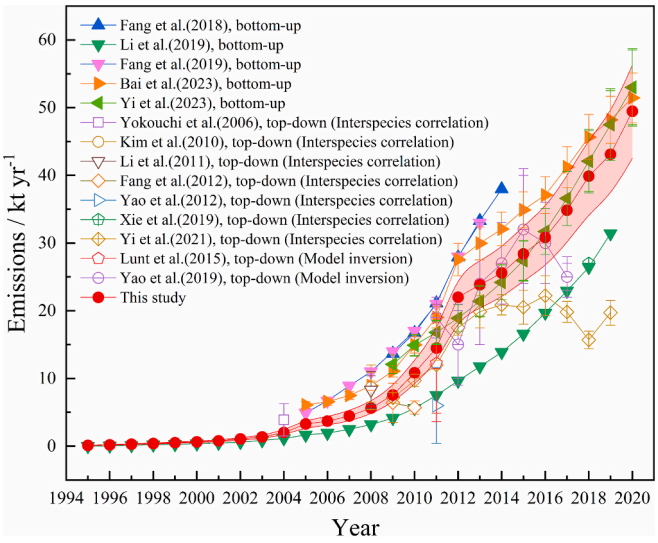

Fig. 5. Derived HFC-134a bottom-up inventory results from this study compared to existing studies. Solid markers indicate emissions derived from bottom-up studies, and the hollow markers indicate emissions derived from top-down studies. The shading and error bars indicate the uncertainty of the emission values.

percentages, ranging from 1% to 8%, as shown in Fig. 4d. Notably, waste disposal emissions have shown a steady increased since 2002, accelerating after 2014, with an average annual growth rate of 23% from 2015 to 2020. Therefore, the implementation and improvement of refrigerant recovery systems aimed at controlling disposal emissions will play a vital role in effectively reducing HFC-134a emissions in sectors like MAC and ICR.

The emissions of HFC-134a will have repercussions for both global climate and aquatic ecology. In terms of the climate impact, China's CO_2-equivalent (CO_2-eq) emissions of HFC-134a increased from 0.1 Mt CO_2-eq in 1995 to 67 Mt CO_2-eq in 2020. Cumulative emissions totaled 494 Mt CO_2-eq (with a range of 420–596 Mt CO_2-eq) from 1995 and 2020, aligning with findings from Bai et al. (2023) and Yi et al. (2023). These emissions in China resulted in an annual increase in direct radiative forcing at an average growth rate of 41%, reaching 4.5 mW/m^2 by 2020, and a temperature increase of 3.6×10^{-3} °C by the same year (Table 1). Detailed calculations are described in section 3 of the methodology.

In terms of impacts on aquatic ecology, the TFA formation potential from the atmospheric degradation of HFC-134a in China has been increasing annually, rising from less than 1 kt yr^{-1} in 1995 to 10 kt yr^{-1} in 2020. Cumulatively, from 1995 to 2020, it totals 74 kt, as shown in Table 1. TFA will continue to accumulate and remain stable in the main sink of the water bodies. The predicted no-effect concentration (PNEC) for freshwater, based on the microalgae Raphidocelis subcapitata, which is the most sensitive freshwater species to TFA, is 560 μg L^{-1} (ECHA, 2024). The current environmental impact of TFA formation potential fro ongoing degradation is considered minor (WMO, 2023). However, it is recommended to regularly reassess the environmental impact of TFA resulting from HFC-134a, especially considering the increasing emissions and uncertainties surrounding the sources and sinks (WMO, 2018, 2011).

3.2. HFC-134a-gridded banks and emissions, and emission validation

The HFC-134a gridded banks and emissions varied significantly across provinces, as illustrated in Fig. 6. The banks and emissions were concentrated in China's eastern region (see the definitions in Table S11), comprising 56% of the national total banks in 2020 (301 kt) and 59% of the national cumulative emissions from 1995 to 2020 (354 kt), respectively. In 2020, the central region accounted for 24% of the total HFC banks, while its cumulative emissions contribution stood at 21%. Conversely, the western region accounted for 13% of the banks and 12% of the cumulative emissions. The northwest region had the smallest share, contributing just 7% of the banks in 2020 and 8% of cumulative emissions over the period. Within the eastern region, Guangdong, Jiangsu, and Shandong provinces emerged as the top three contributors to cumulative emissions from 1995 to 2020, with a total of 98 kt, accounting for 28% of the national total. Additionally, 43 out of the 100 highest emitting grid cells were located in these three provinces. The elevated HFC-134a emissions in these three provinces can be attributed to their comparatively robust GDP and substantial vehicle ownership rates within China, collectively accounting for 24% and 28% of the national total. The high GDP and vehicle ownership rates in these provinces led to increased emissions from both the MAC sector and the ICR sector, contributing 38% and 21% respectively to the national total emissions. In addition, the higher temperatures in Guangdong province compared to other provinces (with summer averages ranging from 24°C to 31°C) (Average temperature in Guangdong, 2022), alongside prolonged usage of car air conditioners per vehicle ownership, are likely significant contributors to the increased emissions of HFC-134a. Moreover, the 100 grid cells with the highest emissions were primarily located in Shandong, Zhejiang, Henan, Hebei, Jiangsu and Anhui, as depicted in Fig. 6d. The gridded bank (Fig. 6c) and emission (Fig. 6d) exhibit a similar spatial distribution. This is because emissions from operation, maintenance, and disposal accounted for approximately 92%-99% of total emissions between 1995 and 2020 (Fig. 4d), and the emissions from all three phases are derived from bank quantities, as shown in Equation 6–16 (Supplementary Information Text Section 1), their distribution patterns closely align.

The simulated mole fractions derived from the NAME model and the HFC-134a gridded inventory (see Fig. S3) closely aligned with the observed mole fractions at nine stations. The majority of observed pollution events coincided with the modeling results. The simulated mole fractions at the Lin'an (LAN) site in eastern China and the Longfengshan (LFS) site in northeastern China might be underestimated because the simulation did not account for emissions from South Korea or other sources outside of China, which could also contribute to the mole fractions at these sites. The goodness of fit between simulated and observed mole fractions was assessed using the NMB and NME values, calculated for each pair of observed and simulated hourly data at each station. According to Emery et al. (2001), NMB within the range of ±50% and NME between 0%–50% are considered reasonable. In this

Table 1
Impacts of HFC-134a Emissions in China: radiative forcing, temperature rise, and TFA formation potential.

	Radiative forcing increases (mW/m^2)	Temperature increases (℃)	TFA formation potential (kt)
1996	1.9×10^{-3}	1.6×10^{-6}	0.0407
2000	2.6×10^{-2}	2.1×10^{-5}	0.1330
2005	0.12	9.8×10^{-4}	0.6895
2015	2.1	1.7×10^{-3}	5.9626
2020	4.5	3.6×10^{-3}	10.050
1995–2020	/	/	74.364

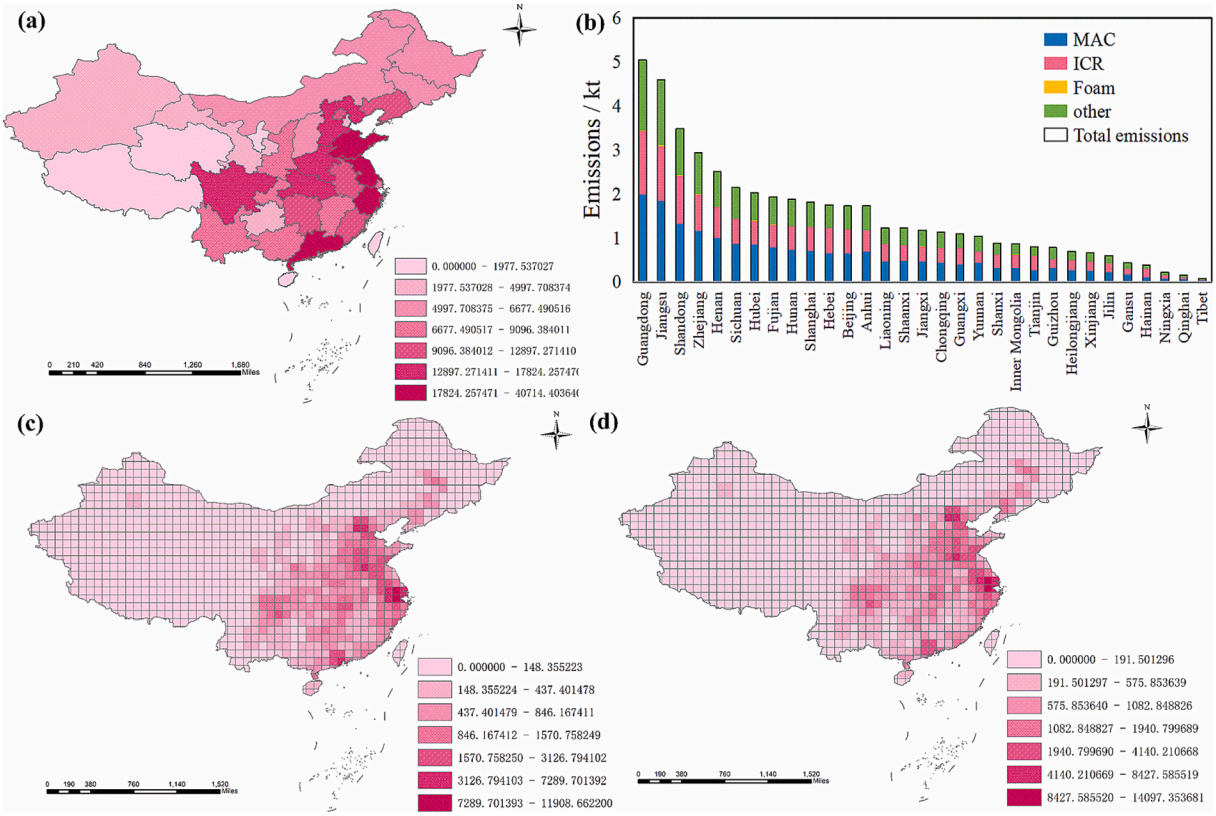

Fig. 6. Distribution of HFC-134a banks and emissions (tonnes) by province and sectors in 2020: (a) spatial distribution of cumulative emissions by province from 1995 to 2020; (b) emissions by provinces and sectors in 2020; (c) spatial distribution of bank of HFC-134a in China in 2020 at a 1° × 1° resolution; (d) spatial distribution of cumulative emissions across China from 1995 to 2020 at a 1° × 1° resolution.

study, the calculated NMB and NME values for each data pair across all sites fell within the range of ±50% and 0%-50%, respectively, indicating a good fit between the simulated and observed mole fractions (Table S6 and S7). For the period 2011–2020, the relative deviation between the annual mean simulated and observed mole fractions at each observation site ranged from −13% to 9%, as detailed in Table S8 (where observations exist). These findings suggest that the simulated values closely align with the observations, supporting the accuracy of the gridded emission inventory of HFC-134a compiled in this study. We observed negative relative deviations between annual mean values at the Shangdianzi (SDZ) and LAN sites in some years, ranging from −8% to −13%, which may be closely linked to the geographical distribution of HFCs production facilities. Most of the HFCs production facilities in China are located in Shandong, Jiangsu, and Zhejiang provinces (Zhejiang Chemical Research Institute, 2016), and the SDZ and LAN sites are located in or near these provinces. Due to the lack of specific production data, we did not account for production emissions in the gridded emission inventory, which may explain the higher bias observed at LAN and SDZ sites.

3.3. *Future emission reduction potential and environmental impacts of HFC-134a*

Under the Pre-KA scenario, assuming China adheres to its domestic controls, the consumption, bank, and emission of HFC-134a would continue to increase annually, reaching 351 kt yr^{-1}, 1,610 kt and 270 kt

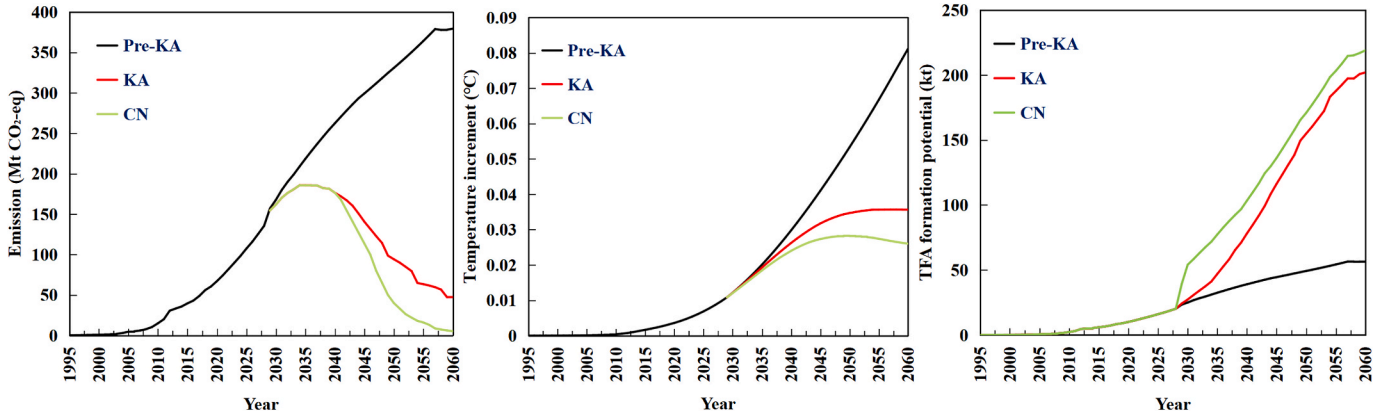

Fig. 7. HFC-134a emissions, temperature increment and TFA formation potential from 2021 to 2060: (a) emissions; (b) temperature increase; and (c) TFA formation potential.

yr^{-1}, respectively, by 2060, as illustrated in Fig. 7. From 2021 to 2060, the cumulative consumption and emissions of HFC-134a are projected to total 8320 kt (12 Gt CO_2-eq) and 7118 kt (10 Gt CO_2-eq), respectively. In addition, the increase in radiative forcing due to HFC-134a emissions in China would amount to 100 mW/m^2 in 2060, leading to a temperature increase of 0.08°C. The atmospheric degradation of HFC-134a could generate up to 1,569 kt of cumulative TFA formation potential between 1995 and 2060. Given TFA's environmental persistence, coupled with its rising emission levels, this compound is expected to lead to substantial environmental buildup over time (Garavagno et al., 2024).

As shown in Fig. 7, under the KA scenario, HFC-134a consumption and emissions would peak at 139 kt yr^{-1} (199 Mt CO_2-eq yr^{-1}) and 131 kt yr^{-1} (185 Mt CO_2-eq yr^{-1}) in 2028 and 2034, respectively. Subsequently, they are projected to decline to 32 kt yr^{-1} (45 Mt CO_2-eq yr^{-1}) and 40 kt yr^{-1} (57 Mt CO_2-eq yr^{-1}) by 2060. In 2060, compared to the Pre-KA scenario, the HFC-134a bank will be reduced to 197 kt, which constitutes only 13% of the Pre-KA scenario. Additionally, the cumulative emissions of HFC-134a projected to be reduced during the period 2021–2060 under the KA scenario amount to 3,603 kt (5,153 Mt CO_2-eq). Meanwhile, under the KA scenario, by 2060, the total radiative forcing increase and temperature rise attributable to the emission of HFC-134a and its alternatives in China will amount to 44 mW/m^2 and 3.6×10^{-2} °C, respectively. This represents a significantly lower climate impact compared to the Pre-KA scenario.

Starting in 2029, if refrigerant and foam recovery is implemented with a 20 % recovery rate, a cumulative emission reduction of 6% is anticipated. If the recovery rate is increased to 80%, the reduction could reach 25%. This comparison clearly shows the importance of increasing the recovery rate of refrigerants and foams to effectively reduce emissions. Assuming that all refrigerant and foams in equipment across all sectors are recovered during the waste disposal stage from 2029 onwards, emissions could be reduced by a cumulative 1,808 kt, representing a 31% reduction. The impact of the recovery rate on emission outcomes is illustrated in Fig. S2. The EU began regulating HFCs in 2006 (EU, 2006), with HFC-134a emissions peaking in 2013—seven years later—and declining steadily thereafter (Annadate et al., 2025). In contrast, China's HFC control efforts began in 2024, and based on our projections, emissions in China are expected to peak in 2034. The observed time lag between the EU and China in terms of emission control implementation and peak emissions may be due to China's substantially higher production and sales volumes, as well as distinct consumption patterns compared to the EU.

However, under the KA scenario by 2060, the cumulative TFA formation potential due to emissions of HFC-134a and its alternatives (HFO-1234yf and R-513A) is projected to reach 3,825 kt. This figure is 2.4 times higher than that observed in the Pre-KA scenario. Notable, HFC-134a emissions accounted for only 19% of the total TFA formation potential, with the majority stemming from the substitution of HFO-1234yf and R-513A. In essence, KA aims to effectively reduce greenhouse gas emissions and their climate impacts. However, it also increases the TFA formation potential, primarily due to the use of alternatives like HFO-1234yf and R-513A. This increase in TFA formation potential poses ecological risks to certain seasonal water bodies, characterized by limited outflow and high evaporation rates, that can lead to the accumulation of TFA.

It is observed that under the KA scenario, China is projected to maintain a bank of 197 kt and emits 40 kt yr^{-1} of HFC-134a by 2060. This poses a challenge for China to achieve its goal of near-zero emissions by 2060, promoting further consideration of the CN scenario, which proposes accelerated reductions, as studied here. Similar to the KA scenario, in the CN scenarios, consumption and emissions of HFC-134a are expected to peak in 2028 and 2034, respectively. However, in the CN scenario, the decline in emissions would be more rapid than in the KA scenario after reaching their respective peaks, eventually reaching to 1.82 kt (2.6 Mt CO_2-eq) by 2060, as shown in Fig. 7. This reduction is estimated to cumulatively avoid greenhouse gas emissions of approximately 1,225 Mt CO_2-eq by 2060 through reductions in HFC-134 consumption. In comparison to the KA scenario, the banks in the CN scenario are projected to undergo further reduction, reaching 4.5 kt in 2060.

In the CN scenario, the projected total radiative forcing increase (or total temperature increase) from emissions of HFC-134a and its alternatives is expected to be lower compared to the KA scenario, totaling 33 mW/m^2 (or 2.6×10^{-2} °C) by 2060. However, as HFC-134a gradually transitions to alternatives like HFO-1234yf and R-513A, the CN scenario is projected to increase the cumulative TFA formation potential in aquatic ecosystem to addition 701 kt between 1995 and 2060, on top of the 3825 kt from KA scenario. Notably, the potential alternatives for HFC-134a in miscellaneous consumption sectors are challenging to identity, and therefore, the listed TFA formation potential does not account for potential emissions from miscellaneous consumption sectors. Consequently, the actual TFA formation potential could be higher than indicated here.

Considering the delayed emission characteristic of HFC-134a, accelerating the phase-out of HFC-134a would effectively mitigate its climate impacts. However, transitioning to alternatives like HFO-1234yf and R-513A in the future may inevitably increase the potential for TFA formation. Regular assessment of the potential risks posed to the water bodies, especially seasonal ones, by HFO-1234yf and R-513A as substitutes for HFC-134a is crucial (WMO, 2023). This is due to the persistence of TFA in water bodies and its significant repercussions for aquatic ecology. The results of this study can assist in providing high spatial resolution inventory data for atmospheric models and evaluating China's contribution to global greenhouse gas emission reduction, and provide a scientific basis for exploring and selecting environmentally sustainable alternatives for HFC-134a, as well as for developing a carbon–neutral emission reduction pathway that accommodates high consumption demands in the future. The spatial characteristics presented in the inventory can provide a key scientific basis for the adjustment of China's regional policies. By illustrating the distribution patterns and trends of emissions across different regions, these spatial features enable policymakers to gain a precise insight into the current status of emissions and potential issues in each region, thereby enhancing the effectiveness of emission reductions measures. The methodological framework developed in this study presents innovative perspectives for future calculation of gridded banks and inventories and their validation on other F-gases and ODS.

A few potential improvements can be considered for future studies. The emission factors used in this study predominantly refer to previous studies and default values prescribed in the IPCC (2006) Guidelines. If localized emission factors become available in the future, more accurate emission estimates could be achieved. Furthermore, provincial-level inventories were derived through apportionment of national inventories using highly relevant allocation parameters in this study. The accuracy of these provincial inventories could be improved if provincial activity data were available for future studies.

CRediT authorship contribution statement

Jing Wu: Writing – review & editing, Supervision, Funding acquisition, Conceptualization. **Tong Wang:** Writing – review & editing, Writing – original draft, Visualization, Validation. **Minde An:** Writing – review & editing, Validation. **Shan Ding:** Writing – original draft, Visualization. **Bo Yao:** Resources. **Luke M. Western:** Writing – review & editing. **Pallav Purohit:** Writing – review & editing. **Zehua Liu:** Methodology. **Zechen Zhang:** Methodology. **Lin Peng:** Supervision, Funding acquisition.

Declaration of competing interest

The authors declare that they have no known competing financial interests or personal relationships that could have appeared to influence

the work reported in this paper.

Acknowledgments

This work was supported by the Natural Science Foundation of China (NSFC) (Grant No. 42375187), Beijing Municipal Natural Science Foundation (Grant No. 8232042), National Key R&D Program of China (Grant No. 2023YFC3709500).

Appendix A. Supplementary material

Supplementary data to this article can be found online at https://doi.org/10.1016/j.envint.2025.109535.

Data availability

Data will be made available on request.

References

An, M.D., Western, L.M., Hu, J.X., Yao, B., Mühle, J., Ganesan, A.L., Prinn, R.G., Krummel, P.B., Hossaini, R., Fang, X.K., O'doherty, S., Weiss, R.F., Young, D., Rigby, M., 2023. Anthropogenic chloroform emissions from china drive changes in global emissions. *Environ. Sci. Tech.* 57, 13925–13936.

An, M.D., Prinn, R.G., Western, L.M., Zhao, X.C., Yao, B., Hu, J.X., Ganesan, A.L., Muehle, J., Weiss, R.F., Krummel, P.B., Odoherty, S., Young, D., Rigby, M., 2024. Sustained growth of sulfur hexafluoride emissions in China inferred from atmospheric observations. *Nat. Commun.* 15.

Annadate, S., Mancinelli, E., Gonella, B., Moricci, F., O'doherty, S., Stanley, K., Young, D., Vollmer, M.K., Cesari, R., Falasca, S., Giostra, U., Maione, M., Arduini, J., 2025. Monitoring the impact of EU F-gas regulation on HFC-134a emissions through a comparison of top-down and bottom-up estimates. *Environ. Sci. Eur.* 37.

Aucott, M.L., Mcculloch, A., Graedel, T.E., Kleiman, G., Midgley, P., Li, Y.F., 1999. Anthropogenic emissions of trichloromethane (chloroform, $CHCl_3$) and chlorodifluoromethane (HCFC-22): Reactive Chlorine Emissions Inventory. *J. Geophys. Res.-Atmos.* 104, 8405–8415.

Average temperature in Guangdong [Online]. Available: https://www.tianqi.com/qiwen/city_guangdong/. (Accessed October 2022).

Bai, F., An, M., Wu, J., Fang, X., Jiang, P., Yao, B., Zhao, X., Xiang, X., Chen, Z., Hu, J., 2023. Pathway and cost-benefit analysis to achieve China's zero hydrofluorocarbon emissions. *Environ. Sci. Tech.* 57, 6474–6484.

Berends, A.G., Boutonnet, J.C., De Rooij, C.G., Thompson, R.S., 1999. Toxicity of trifluoroacetate to aquatic organisms. *Environ. Toxicol. Chem.* 18, 1053–1059.

David, L.M., Barth, M., Höglund-Isaksson, L., Purohit, P., Velders, G.J.M., Glaser, S., Ravishankara, A.R., 2021. Trifluoroacetic acid deposition from emissions of HFO-1234yf in India, China, and the Middle East. *Atmos. Chem. Phys.* 21, 14833–14849.

Ding, S., Wu, J., Wang, J., Ma, T.F., Zhang, D.Y., Hu, D.M., Zhang, Y.L., 2023. Establishment of HFC-134a Emission Inventory in the North China Plain from 1995 to 2020. Atmosphere 14.

Doll, C.N.H., Muller, J.P., Elvidge, C.D., 2000. Night-time imagery as a tool for global mapping of socioeconomic parameters and greenhouse gas emissions. *Ambio* 29, 157–162.

EDGAR (Emissions Database for Global Atmospheric Research), 2023. Community GHG Database, a collaboration between the European Commission, Joint Research Centre (JRC), the International Energy Agency (IEA). EDGAR F-GASES version 8.0 ed. European Commission, JRC.

ECHA, 2024. European Chemical Agency. Registration dossier for trifluoroacetic acid. EC number: 200-929-3; CAS number: 76-05-1 [Online]. European Chemical Agency. Available: https://chem.echa.europa.eu/100.000.846/dossier-view/60cec416-2eda-4340-98bb-abde81256cda/IUC5-ddcd67f1-925d-4d99-9f9b-ccc88b5baf6d_eefba020-ad0c-4e61-b30f-64b6882cbf68. (Accessed 13 May 2024).

Emery, C., Tai, E., Yarwood, G., 2001. Enhanced meteorological modeling and performance evaluation for two Texas ozone episodes. In: *Prepared for the Texas Natural Resource Conservation Commission, by ENVIRON International Corporation*, p. 161.

EU (European Union), Directive 2006/40/EC of the European parliament and of the council of 17 May 2006 relating to emissions from air-conditioning systems in motor vehicles. Official J. EU L161, 12-18. Available at: https://eur-lex.europa.eu/legal-content/EN/TXT/?uri=CELEX%3A32006L0040.

Fang, X.K., Velders, G.J.M., Ravishankara, A.R., Molina, M.J., Hu, J., Prinnt, R.G., 2016. Hydrofluorocarbon (HFC) emissions in China: an inventory for 2005-2013 and projections to 2050. *Environ. Sci. Tech.* 50, 2027–2034.

Fang, X.K., Wu, J., Su, S., Han, J., Wu, Y., Shi, Y., Wan, D., Sun, X., Zhang, J., Hu, J., 2012. Estimates of major anthropogenic halocarbon emissions from China based on interspecies correlations. *Atmos. Environ.* 62, 26–33.

Fang, X.K., Park, S., Saito, T., Tunnicliffe, R., Ganesan, A.L., Rigby, M., Li, S.L., Yokouchi, Y., Fraser, P.J., Harth, C.M., Krummel, P.B., Muhle, J., O'doherty, S., Salameh, P.K., Simmonds, P.G., Weiss, R.F., Young, D., Lunt, M.F., Manning, A.J., Gressentl, A., Prinn, R.G., 2019. Rapid increase in ozone-depleting chloroform emissions from China. *Nat. Geosci.* 12, 89.

Fang, X.K., Ravishankara, A.R., Velders, G.J.M., Molina, M.J., Su, S.S., Zhang, J.B., Hu, J.X., Prinn, R.G., 2018. Changes in emissions of ozone-depleting substances from china due to implementation of the Montreal protocol. *Environ. Sci. Tech.* 52, 11359–11366.

Freeling, F., Scheurer, M., Koschorreck, J., Hoffmann, G., Ternes, T.A., Nodler, K., 2022. Levels and Temporal Trends of Trifluoroacetate (TFA) in archived plants: evidence for increasing emissions of gaseous TFA precursors over the last decades. *Environ. Sci. Technol. Lett.* 9, 400–405.

Garavagno, M.D.L.A., Holland, R., Khan, M.A.H., Orr-Ewing, A.J., Shallcross, D.E., 2024. Trifluoroacetic acid: toxicity, sources, sinks and future prospects. *Sustainability* 16, 2382.

Gidden, M.J., Riahi, K., Smith, S.J., Fujimori, S., Luderer, G., Kriegler, E., Van Vuuren, D. P., Van Den Berg, M., Feng, L., Klein, D., Calvin, K., Doelman, J.C., Frank, S., Fricko, O., Harmsen, M., Hasegawa, T., Havlik, P., Hilaire, J., Hoesly, R., Horing, J., Popp, A., Stehfest, E., Takahashi, K., 2019. Global emissions pathways under different socioeconomic scenarios for use in CMIP6: a dataset of harmonized emissions trajectories through the end of the century. *Geosci. Model Dev.* 12, 1443–1475.

Godwin, D.S., 2012. Demand for ozone-depleting substances and hydrofluorocarbons estimated by a Tier 2 emission inventory model compared to top-down chemical consumption data for the US. *J. Integr. Environ. Sci.* 9, 81–95.

Harnisch, J., De Jager, D., Gale, J., Stobbe, O., 2002. Halogenated compounds and climate change: Future emission levels and reduction costs. *Environ. Sci. Pollut. Res.* 9, 369–374.

IPCC (Intergovernmental Panel on Climate Change). 2006. 2006 IPCC Guidelines for National Greenhouse Gas Inventories, vol. 3. Industrial Process and Product Use. Institute for Global Environmental Strategies (IGES): Japan.

IPCC (Intergovernmental Panel on Climate Change), 2021. Climate Change 2021: The Physical Science Basis. Cambridge, United Kingdom and New York: Cambridge University Press.

Jones, A., Thomson, D., Hort, M., Devenish, B., 2007. The U.K. Met Office's Next-Generation Atmospheric Dispersion Model, NAME III. *Air Pollution Modeling and Its Application XVII.* Borrego, C., Norman, AL: Springer, Boston, MA.

Kim, J., Li, S., Kim, K.R., Stohl, A., Muehle, J., Kim, S.K., Park, M.K., Kang, D.J., Lee, G., Harth, C.M., Salameh, P.K., Weiss, R.F., 2010. Regional atmospheric emissions determined from measurements at Jeju Island, Korea: halogenated compounds from China. Geophys. Res. Lett. 37.

Li, S., Kim, J., Kim, K.R., Muhle, J., Kim, S.K., Park, M.K., Stohl, A., Kang, D.J., Arnold, T., Harth, C.M., Salameh, P.K., Weiss, R.F., 2011. Emissions of halogenated compounds in East Asia determined from measurements at Jeju Island, Korea. *Environ. Sci. Tech.* 45, 5668–5675.

Li, Y.X., Zhang, Z.Y., An, M.D., Gao, D., Yi, L.Y., Hu, J.X., 2019. The estimated schedule and mitigation potential for hydrofluorocarbons phase-down in China. *Adv. Clim. Chang. Res.* 10, 174–180.

Jin, L.Z., Shao, Z.Y., Mao, X.L., Miller, J., He, H., Isenstadt, A., 2021. Opportunities and pathways to decarbonize China's transportation sector during the Fourteenth Five-Year Plan period and beyond. Int. Council Clean Transp. (ICCT).

Luecken, D.J., Waterland, R.L., Papasavva, S., Taddonio, K.N., Hutzell, W.T., Rugh, J.P., Andersen, S.O., 2010. Ozone and TFA Impacts in North America from Degradation of 2,3,3,3-Tetrafluoropropene (HFO-1234yf), A Potential Greenhouse Gas Replacement. *Environ. Sci. Tech.* 44, 343–348.

Lunt, M.F., Rigby, M., Ganesan, A.L., Manning, A.J., Prinn, R.G., O'doherty, S., Muehle, J., Harth, C.M., Salameh, P.K., Arnold, T., Weiss, R.F., Saito, T., Yokouchi, Y., Krummel, P.B., Steele, L.P., Fraser, P.J., Li, S., Park, S., Reimann, S., Vollmer, M.K., Lunder, C., Hermansen, O., Schmidbauer, N., Maione, M., Arduini, J., Young, D., Simmonds, P.G., 2015. Reconciling reported and unreported HFC emissions with atmospheric observations. *PNAS* 112, 5927–5931.

Ministry of Ecology and Environment of the People's Republic of China, 2023. The Third Biennial Update Report on Climate Change of the People's Republic of China. Beijing: Government of the People's Republic of China.

Montzka, S.A., Mcfarland, M., Andersen, S.O., Miller, B.R., Fahey, D.W., Hall, B.D., Hu, L., Siso, C., Elkins, J.W., 2015. Recent trends in global emissions of hydrochlorofluorocarbons and hydrofluorocarbons: reflecting on the 2007 adjustments to the Montreal protocol. *J. Phys. Chem.* 119, 4439–4449.

National Bureau of Statistics of China, 2020. China Statistical Yearbook 2020 (in Chinese). China Statistics Press.

Papasavva, S., Luecken, D.J., Waterland, R.L., Taddonio, K.N., Andersen, S.O., 2009. Estimated 2017 refrigerant emissions of 2,3,3,3-tetrafluoropropene (HFC-1234yf) in the United States resulting from automobile air conditioning. *Environ. Sci. Tech.* 43, 9252–9259.

People's Government of the People's Republic of China, 2021. Opinions of the State Council on the complete, accurate and comprehensive implementation of the new development concept to do a good job in carbon peak carbon neutrality.

Purohit, P., Borgford-Parnell, N., Klimont, Z., Höglund-Isaksson, L., 2022. Achieving Paris climate goals calls for increasing ambition of the Kigali Amendment. *Nat. Clim. Chang.* 12, 339–342.

Purohit, P., Höglund-Isaksson, L., 2017. Global emissions of fluorinated greenhouse gases 2005-2050 with abatement potentials and costs. *Atmos. Chem. Phys.* 17, 2795–2816.

Purohit, P., Höglund-Isaksson, L., Dulac, J., Shah, N., Wei, M., Rafaj, P., Schöpp, W., 2020. Electricity savings and greenhouse gas emission reductions from global phase-down of hydrofluorocarbons. *Atmos. Chem. Phys.* 20, 11305–11327.

Rigby, M., Prinn, R.G., O'doherty, S., Montzka, S.A., Mcculloch, A., Harth, C.M., Mühle, J., Salameh, P.K., Weiss, R.F., Young, D., Simmonds, P.G., Hall, B.D., Dutton, G.S., Nance, D., Mondeel, D.J., Elkins, J.W., Krummel, P.B., Steele, L.P., Fraser, P.J., 2013. Re-evaluation of the lifetimes of the major CFCs and CH3CCl3 using atmospheric trends. *Atmos. Chem. Phys.* 13, 2691–2702.

Roh, S.A., Kim, W.H., Jung, D.S., Hong, B.K., 2019. Thermal destruction of HFC-134a in pilot-, and full-scale gasification systems. *J. Energy Inst.* 92, 1842–1851.
Sharma, M., Chaturvedi, V., Purohit, P., 2017. Long-term carbon dioxide and hydrofluorocarbon emissions from commercial space cooling and refrigeration in India: a detailed analysis within an integrated assessment modelling framework. *Clim. Change* 143, 503–517.
Smith, C., Nicholls, Z.R.J., Armour, K., Collins, W., Forster, P., Meinshausen, M., Palmer, M.D., Watanabe, M., 2021. The Earth's Energy Budget, Climate Feedbacks, and Climate Sensitivity Supplementary Material. In: Climate Change 2021: The Physical Science Basis. Contribution of Working Group I to the Sixth Assessment Report of the Intergovernmental Panel on Climate Change.
UNEP (United Nations Environment Programme), 2024. UN Environment Programme ozone secretariat Data [Online]. Available: https://ozone.unep.org/countries/data?report_type=0&group%5B0%5D=10&period_start=1986&period_end=2023&output_type=odp-CO2e-tonnes. (Accessed 14 May 2024).
UN, 2025. United Nations: Chapter XXVII – Environment (2.f Amendment to the Montreal Protocol on Substances that Deplete the Ozone Layer), Treaty Section [Online]. Office of Legal Affairs, United Nations, New York. Available: https://treaties.un.org/Pages/ViewDetails.aspx?src=IND&mtdsg_no=XXVII-2-f&chapter=27&clang=_en. (Accessed 27 March 2025).
Velders, G.J.M., Solomon, S., Daniel, J.S., 2014. Growth of climate change commitments from HFC banks and emissions. *Atmos. Chem. Phys.* 14, 4563–4572.
Kotamarthi, V.-R., Rodriguez, J.-M., Ko, M.K.W., et al., 1998. Trifluoroacetic acid from degradation of HCFCs and HFCs: a three-dimensional modeling study. J. Geophys. Res.-Atmos. 103 (D5), 5747–5758.
Wang, Z., 2018. Research on Emissions, Atmospheric Processes and Product Distribution of Fluorinated Olefins. Peking University (in Chinese).
Wei, W., 2011. Current Status and Future Trends of Volatile Organic Compounds Emissions from Anthropogenic Sources in China. Tsinghua University (in Chinese).
UNEP, 2020. Handbook for the Montreal Protocol on substances that deplete the ozone layer, Ozone Secretariat. Nairobi, Kenya.
WMO (World Meteorological Organization), 2011. Scientific Assessment of Ozone Depletion: 2010, Global Ozone Research and Monitoring Project–Report No. 52. Geneva.
WMO (World Meteorological Organization), 2018. Scientific Assessment of Ozone Depletion: 2018, Global Ozone Research and Monitoring Project–Report No. 58. Geneva.
WMO (World Meteorological Organization), 2023. Scientific Assessment of Ozone Depletion: 2022, GAW Report No. 278. Geneva.
Wu, J., Ding, S., Fang, X.K., Bai, F.L., Li, T., Wang, J., Zhang, D.Y., Ma, T.F., Yi, L.Y., Hu, J.X., 2023. Banks, emissions, and Environmental Impacts of China's ozone depletion substances and hydrofluorocarbon substitutes during 1980–2020. Sci. Total Environ. 882.
Wu, J., Li, T., Wang, J., Zhang, D., Peng, L., 2022. Establishment of HCFC-22 national-provincial-gridded emission inventories in China and the analysis of emission reduction potential. *Environ. Sci. Tech.* 56, 814–822.
Wu, J., Martin, J.W., Zhai, Z., Lu, K., Li, L., Fang, X., Jin, H., Hu, J., Zhang, J., 2014. Airborne trifluoroacetic acid and its fraction from the degradation of HFC-134a in Beijing, China. *Environ. Sci. Tech.* 48, 3675–3681.
Xiang, X.Y., Zhao, X.C., Jiang, P.N., Wang, J., Gao, D., Bai, F.L., An, M.D., Yi, L.Y., Wu, J., Hu, J.X., 2022. Scenario analysis of hydrofluorocarbons emission reduction in China's mobile air-conditioning sector. *Adv. Clim. Chang. Res.* 13, 578–586.
Xie, W., Yao, B., Quan, W., Fang, S., Ma, Z., Zhou, H., Dong, F., Zhou, L., He, D., Shi, Q., Chen, L., 2019. Online observation of hydrofluorocarbons at the Shangdianzi atmospheric background station in Beijing. *Chin. Environ. Sci.* 39, 4941–4949.
Xu, Y., Zaelke, D., Velders, G.J.M., Ramanathan, V., 2013. The role of HFCs in mitigating 21st century climate change. *Atmos. Chem. Phys.* 13, 6083–6089.
Yang, H., 2010. Consumption and Emission Inventory and Prediction of HCFC-22 in China. Peking university (in Chinese).
Yao, B., Fang, X., Vollmer, M.K., Reimann, S., Chen, L., Fang, S., Prinn, R.G., 2019. China's hydrofluorocarbon emissions for 2011–2017 inferred from atmospheric measurements. *Environ. Sci. Technol. Lett.* 6, 479–486.
Yao, B., Vollmer, M.K., Zhou, L.X., Henne, S., Reimann, S., Li, P.C., Wenger, A., Hill, M., 2012. In-situ measurements of atmospheric hydrofluorocarbons (HFCs) and perfluorocarbons (PFCs) at the Shangdianzi regional background station, China. *Atmos. Chem. Phys.* 12, 10181–10193.
Yi, L., Wu, J., An, M., Xu, W., Fang, X., Yao, B., Li, Y., Gao, D., Zhao, X., Hu, J., 2021. The atmospheric concentrations and emissions of major halocarbons in China during 2009-2019*. *Environ. Pollut.* 284.
Yi, L., Xiang, X., Zhao, X., Xu, W., Jiang, P., Hu, J., 2023. Atmospheric observation and emission of HFC-134a in China and its four cities. *Environ. Sci. Tech.* 57, 4732–4740.
Yokouchi, Y., Taguchi, S., Saito, T., Tohjima, Y., Tanimoto, H., Mukai, H., 2006. High frequency measurements of HFCs at a remote site in east Asia and their implications for Chinese emissions. *Geophys. Res. Lett.* 33.
Zhai, Z., Wu, J., Hu, X., Li, L., Guo, J., Zhang, B., Hu, J., Zhang, J., 2015. A 17-fold increase of trifluoroacetic acid in landscape waters of Beijing, China during the last decade. *Chemosphere* 129, 110–117.
Zhang, H., Shen, R., Zhang, X., 2022. Implications and pathways of China's carbon neutrality: a review (in Chineses). *Clim. Change Res.* 18, 240–252.
Zhejiang Chemical Research Institute. 2016. Hydrofluorocarbons (HFCs) in China's Fluorochemical Industry Gradual Reduction Trend Study. (in Chinese).